Measurement of Electron-Impact-Excitation Cross Sections for Very Highly Charged Ions

R. E. Marrs, M. A. Levine, D. A. Knapp, and J. R. Henderson
Lawrence Livermore National Laboratory, University of California, Livermore, California 94550
(Received 6 November 1987)

We report the first measurements of electron-impact-excitation cross sections for very highly charged ions (Ba^{46+}), and introduce a powerful new technique for studying these ions. Approximately 2×10^4 Ba^{46+} ions/cm were trapped inside the space charge of an $\simeq$120-mA electron beam and their x-ray emission spectra observed with Si(Li) and Bragg-crystal-diffraction spectrometers. Cross sections for several $n=3$ levels excited from the neonlike Ba^{46+} ground state were measured relative to radiative recombination on the same ions.

PACS numbers: 34.80.Kw

The interaction of highly charged ions with electrons, as well as their spectroscopic properties, are important for the understanding of atomic structure in the high-field (high Z) limit where relativistic and QED effects are important. At present there are a few measurements of ionization cross sections for charge states up to $q\lesssim+50$,[1] but direct measurements of electron-impact excitation (IE), dielectronic recombination (DR), and radiative recombination (RR) cross sections have been possible only for $q\lesssim+6$ with use of the available techniques of crossed or merged beams.[2,3]

We have developed a new technique which, for the first time, makes it possible to measure all of these cross sections for highly charged ions. The technique consists of trapping ions inside an electron beam compressed to a density of order 2000 A/cm^2. Cross sections are determined from x-ray spectroscopy of the trapped ions excited by the electron beam. Because the target ions are prepared in a single charge state and the electron beam is monoenergetic, it is possible to unravel all of the separate cross sections which contribute to x-ray emission.

The method of successive ionization of ions trapped in an electron beam is also used in the electron-beam ion sources (EBIS) developed to provide highly charged ions for injection into accelerators.[1] There is one published observation of x rays from an EBIS (from DR on Ar^{14+}).[4] However, the EBIS sources have not proved suitable for x-ray spectroscopy of more highly charged ions. In contrast to the EBIS, our device uses a different and much smaller geometry which is optimized for x-ray spectroscopy.[5] In this Letter we describe our electron-beam ion trap and present measurements of the IE cross sections (relative to RR on the same ions) for several $n=2$ to $n=3$ transitions in the neonlike Ba^{46+} ion.

As shown schematically in Fig. 1, the ion trap consisted of a copper cylinder with an inside diameter of 10 mm in the central trap region and 3 mm at the ends. The electron beam, which follows the central magnetic-field line of the superconducting Helmholtz coils, was injected vertically from a Pierce gun. The beam was adiabatically compressed in the Helmholtz-coil field. The electron currents used ranged from 60 to 120 mA, and the beam radius at the peak magnetic field of 3 T was roughly 35 μm.

The electron-ion interaction energy was determined by the output voltage of a precision high-voltage regulator that biased the drift tube. Because of the space-charge potential of the beam, the actual electron energy was suppressed by about 170 V in the (larger diameter) center of the drift tube and 130 V in the (smaller diameter) ends with respect to the drift-tube bias voltage. This $\simeq$40-V potential difference trapped ions axially, while the $\simeq$15-V potential difference between the center and outer radius of the beam trapped the ions radially. An upper limit of 70 eV FWHM for the beam energy spread was determined from the width of DR resonances observed in an electron excitation function with Ni^{26+} target ions. This width is not large enough to affect the present IE measurements.

The drift tube and the surrounding Helmholtz-coil assembly were operated at a temperature of 4 K. X rays

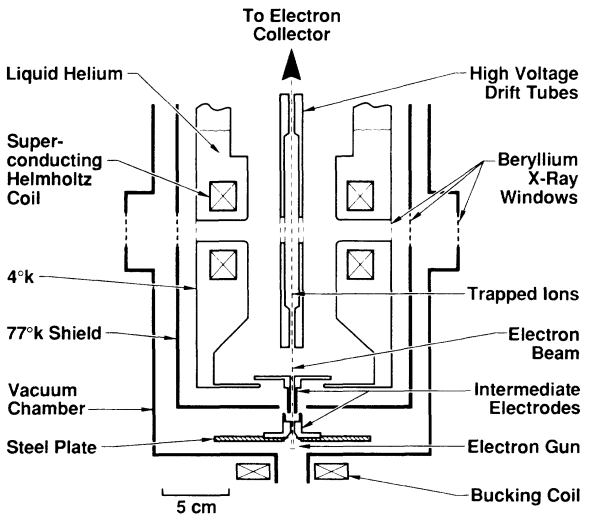

FIG. 1. Electron-beam ion-trap arrangement.

were observed at 90° to the electron beam (in the midplane of the Helmholtz coils) with two spectrometers: a 5-mm-thick×6-mm-diam Si(Li) detector and a Bragg-diffraction spectrometer consisting of a flat pentaerythritol crystal and a position-sensitive proportional counter filled with a Xe-CH_4 gas mixture.

Barium atoms (along with an unwanted tungsten contaminant) were introduced into the space between the drift tube and the intermediate electrodes (see Fig. 1) by evaporation and sputtering from the dispenser-type cathode of the electron gun. Approximately 2×10^4 Ba^{46+} ions/cm were trapped inside the electron beam. This neutralized about 1% of the electron-beam space charge. The trapping mechanism is complicated and consists of a balance between the accretion and loss of barium ions as well as background ions from residual gases in the vacuum chamber. For the measurements reported here the trap was operated in a continuous mode, which requires a substantial loss rate of low-charge-state ions in order to balance the heating of the trapped Ba^{46+} ions by Coulomb collisions with the beam electrons. The barium charge state was selected by our keeping the electron energy between the 3.66- and 8.33-keV ionization potentials of Ba^{45+} and Ba^{46+}.

The neonlike Ba^{46+} configuration was selected for study because of the simplicity of a closed-shell configuration and the experimental convenience of the electron and x-ray energies involved. In Ba^{46+} there are 36 $n=3$ singly excited levels spanning the energy range from 4.56 to 5.64 keV. The crystal spectrometer was set to cover this x-ray energy range. X-ray spectra were obtained at electron energies of $E_e=5.69$ and 8.20 keV, chosen to avoid the strongest DR resonances. The lower energy is just above threshold for the highest $n=3$ level, and the higher energy is just below the ionization potential for Ba^{46+}. Since both energies are above threshold for direct excitation of the highest $n=3$ level, DR does not involve an $n=3$ electron. However, the $n=2$ to $n=3$ x-ray intensities could still be slightly affected by cascade from $n>3$ DR configurations.

A typical Si(Li) spectrum is shown in Fig. 2. The weak features between 6 and 8 keV are due to DR onto Ba^{46+} or tungsten in several charge states and RR to excited states. The feature just above 9 keV is RR to the five unresolved $n=3$ levels in Ba^{45+}. A high-resolution crystal-diffraction spectrum obtained in a longer (5 h) run at the same electron energy is shown in Fig. 3.

The ionization balance between Ba^{46+} and Ba^{45+} was inferred from the relative intensities of the Ba^{45+} satellite lines in the crystal spectra. The upper levels for these transitions are excited by inner-shell excitation from the $(2s^22p^63s)_{1/2}$ Ba^{45+} ground state. They were identified from their calculated energies and oscillator strengths, and have small ($\lesssim10\%$) Auger decay branches. The assumption that the observed x-ray intensity ratio of (Ba^{45+} satellite)/(Ba^{46+} parent) is equal to the Ba^{45+}/Ba^{46+} ionization balance implies $\simeq15\%$ Ba^{45+} at $E_e=5.69$ keV and $\simeq9\%$ Ba^{45+} at $E_e=8.20$ keV. (This ionization balance is roughly consistent with that expected from the ratio of the Ba^{46+} RR and the estimated Ba^{45+} ionization cross sections.) Since both the IE and RR cross sections are expected to differ only

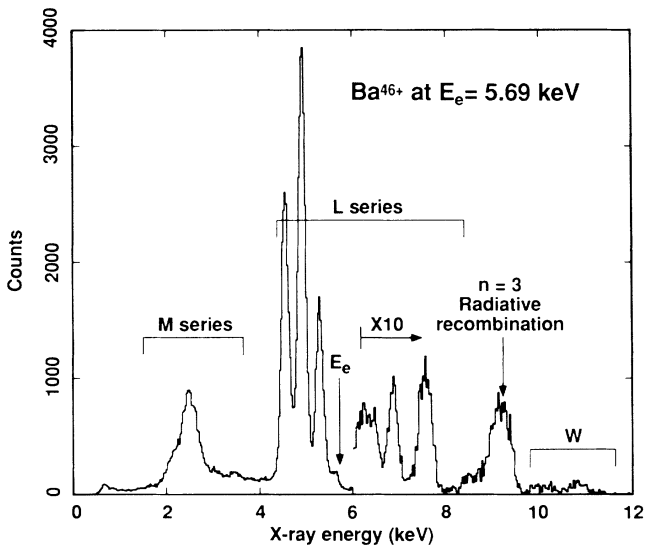

FIG. 2. Si(Li) spectrum. The spectrum is cut off below $\simeq2.5$ keV by absorption in the beryllium windows. The feature labeled W is attributed to RR onto tungsten ions, which were contaminant in the trap. The spectrum has been multiplied by 10 above 6 keV for display purposes.

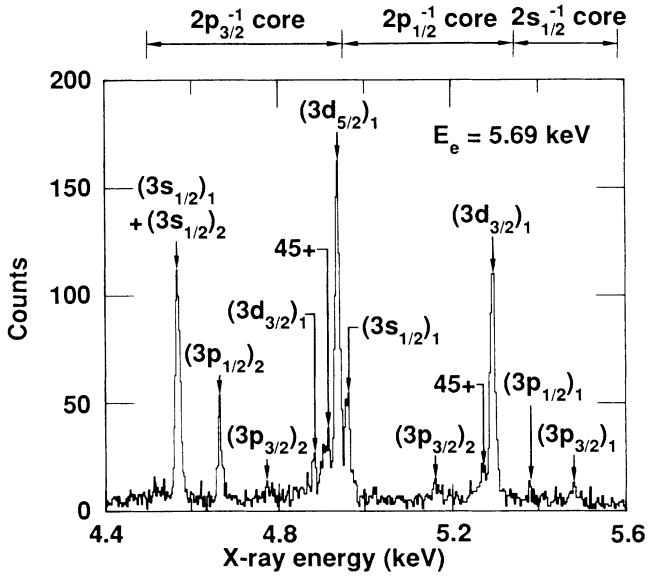

FIG. 3. Crystal-diffraction spectrum. Lines are identified by (nl_j) of the excited electron and total angular momentum J. The spectral regions indicated by bars corresponds to the three different core configurations for the identified lines. The two features labeled 45+ are satellite lines in Ba^{45+}.

slightly between Ba^{46+} and Ba^{45+}, the Ba^{45+} does not have a large effect on the measured IE-RR cross-section ratio for Ba^{46+}.

By combination of the information in the Si(Li) and crystal x-ray spectra it is possible to obtain experimental values for some of the $n=2$ to $n=3$ IE cross sections normalized to the RR cross section, which can be calculated more reliably. We do this here for the three strongest L x rays since they are resolved in the Si(Li) spectrum. The yields of these three x-ray lines and the (unresolved) $n=3$ RR lines were extracted from the Si(Li) spectrum by least-squares fitting. The contributions of the weaker Ba^{46+} L x-ray lines were determined from the higher-resolution crystal spectra and subtracted from the Si(Li) x-ray yields. Small corrections were made for differential absorption in the beryllium windows. For the RR cross sections we use values of $(d\sigma/d\Omega)(90°)=1.99\times10^{-23}$ cm^2/sr at $E_e=5.69$ keV and 1.11×10^{-23} cm^2/sr at $E_e=8.20$ keV. These values are the sums of the separate RR cross sections to the five sodiumlike $n=3$ levels calculated by Scofield using a relativistic distorted-wave code.[6] It was necessary to subtract a tungsten background feature from the shoulder of the Ba^{46+} RR x-ray yield (see Fig. 2) for both electron energies. The accuracy of this background subtraction was confirmed by our retuning the ion trap in a way which increased the tungsten background by a factor of 3 and obtaining consistent results.

The decay scheme for the relevant Ba^{46+} levels is shown in Fig. 4. Direct excitation from the ground state dominates the feeding of all the levels chosen for study. Small corrections for other feeding, as shown in Fig. 4, were made with use of theoretical collision strengths[7] and radiative decay rates[8] for all 88 $n=3$ and $n=4$ levels. The three $J=0$ levels, forbidden to decay to the ground state, are responsible for essentially all of the 4568-eV $(2p_{3/2}^{-1}3s_{1/2})_1$ x-ray yield through their $\Delta n=0$ decays to that level. It is their summed IE cross sections which we measure. Calculated $E1$ transition rates were used to determine the $J=0$ decay branching ratios.[8] The 4568-eV x-ray yield was corrected for a calculated unresolved contribution from the 4562-eV $(2p_{3/2}^{-1}3s_{1/2})_2$ decay which amounted to 31% and 28% at $E_e=5.69$ and 8.20 keV, respectively. This is the largest theory-dependent correction to our data.

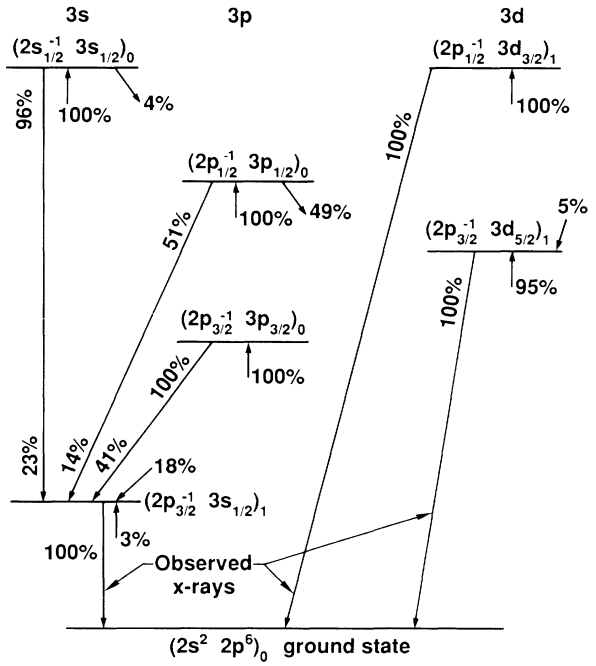

FIG. 4. Diagram of the Ba^{46+} levels involved in the cross-section measurements. The decay branching ratios and feeding ratios shown for the excited levels are derived from theoretical rates at $E_e=5.69$ keV. Upward arrows indicate electron IE from the ground state. Downward arrows indicate cascade feeding and decay, which sometimes involves levels that are not shown.

Table I summarizes our results and compares them with two different theoretical calculations: a Coulomb-Born-exchange method with relativistic effects treated as a perturbation,[9] and a fully relativistic distorted-wave calculation.[7] The measured values in Table I are 4π sr times the differential cross sections at an x-ray angle of 90° with respect to the electron beam. For the $J=0$ decays this is the total IE cross section, but the remaining two ($E1$) transitions in Table I may have a nonisotropic angular distribution. Since x-ray measurements were possible only at 90°, a correct accounting of the angular distributions for the $E1$ transitions will have to await either future differential cross-section calculations or mea-

TABLE I. Comparison of measured and theoretical electron IE cross sections for neonlike Ba^{46+}. Units are 10^{-21} cm^2.

		$E_e=5.69$ keV			$E_e=8.20$ keV		
Level	Energy (eV)	σ Theory[a]	σ Theory[b]	$4\pi\frac{d\sigma}{d\Omega}(90°)$ Measured	σ Theory[a]	σ Theory[b]	$4\pi\frac{d\sigma}{d\Omega}(90°)$ Measured
Sum $J=0$		2.58	2.60	2.50 ± 0.35	1.89	1.94	2.27 ± 0.32
$(2p_{3/2}^{-1}3d_{5/2})_1$	4937	3.44	3.56	3.98 ± 0.56	2.99	3.23	3.30 ± 0.46
$(2p_{1/2}^{-1}3d_{3/2})_1$	5295	2.42	2.00	2.12 ± 0.30	2.10	1.82	1.82 ± 0.25

[a]Obtained by interpolation from values tabulated in Ref. 9 for $Z=54$ and 58 at different collision energies.
[b]Relativistic distorted-wave calculation for Ba^{46+}, Ref. 7.

surements at other angles.

The largest experimental uncertainty in our cross sections, which we estimate to be about $\pm 10\%$, is due to the tungsten background subtraction. When this is added in quadrature with estimated uncertainties due to the Ba^{45+} fraction, background under the $n=2$ to $n=3$ lines, subtraction of weak Ba^{46+} lines, and counting statistics, then an overall instrumental uncertainty of $\pm 14\%$ is obtained for the IE-RR cross-section ratios. The RR code used for normalization of the IE cross sections presented in the table has been compared to measurements of photoionization of inner-shell electrons in heavy neutral atoms (the inverse of RR) at electron and photon energies similar to those in the present Ba^{46+} measurements. The agreement is within a few percent.[6] This comparison suggests that our IE cross sections contain an additional uncertainty on the order of $\pm 5\%$ due to the RR normalization. The uncertainties listed in the table correspond to $\pm 14\%$.

We have also obtained crystal-diffraction spectra at $E_e=7.94$ and 8.40 keV and have done a more extensive comparison of relative $n=2$ to $n=3$ line intensities. The theoretical excitation and cascade decay rates of all $n=3$ and $n=4$ levels were combined to produce theoretical x-ray line intensities. No obvious discrepancies between the theoretical and measured relative intensities were observed for any of the Ba^{46+} L x rays. This consistency among results at four different energies suggests that the IE cross sections are relatively free from the influence of DR resonances.

In conclusion, our Ba^{46+} electron IE measurements illustrate the effectiveness of the electron-beam ion trap for the study of very highly charged ions. The measured IE cross sections, which are the first for highly charged ions, support existing theoretical calculations. Other experiments now in preparation will provide measurements of DR cross sections and precise excitation energies.

We thank K. J. Reed for providing calculated collision strengths and J. H. Scofield for calculating the radiative recombination cross sections. Excellent contributions to the design of the apparatus by R. Wolgast and W. Hearn are gratefully acknowledged. We thank R. J. Fortner for his encouragement and support. This work was performed under the auspices of the U.S. Department of Energy by Lawrence Livermore National Laboratory under Contract No. W-7405-Eng-48.

[1]E. D. Donets, Phys. Scr. **T3**, 11 (1983); E. D. Donets and V. P. Ovsyannikov, Zh. Eksp. Teor. Fiz. **80**, 916 (1981) [Sov. Phys. JETP **53**, 466 (1981)].

[2]D. Gregory, G. H. Dunn, R. A. Phaneuf, and D. H. Crandall, Phys. Rev. A **20**, 410 (1979).

[3]P. F. Dittner, S. Datz, P. D. Miller, P. L. Pepmiller, and C. M. Fou, Phys. Rev. A **35**, 3668 (1987).

[4]J. P. Briand, P. Charles, J. Arianer, H. Laurent, C. Goldstein, J. Dubau, M. Loulergue, and F. Bely-Dubau, Phys. Rev. Lett. **52**, 617 (1984).

[5]M. A. Levine, R. E. Marrs, J. R. Henderson, D. A. Knapp, and M. B. Schneider, Phys. Scr. (to be published).

[6]E. B. Saloman, J. H. Hubbell, and J. H. Scofield, At. Data Nucl. Data Tables **38**, 1 (1988).

[7]K. J. Reed, Phys. Rev. A **37**, 1791 (1988).

[8]J. H. Scofield, unpublished. $E1$, $M1$, $E2$, and $M2$ rates were obtained from the RAC relativistic atomic structure code used at Lawrence Livermore National Laboratory for many years.

[9]H. Zhang, D. H. Sampson, R. E. H. Clark, and J. B. Mann, At. Data Nucl. Data Tables **37**, 17 (1987).